J. Fluid Mech. (1973), *vol.* 57, *part* 4, *pp.* 769–784
Printed in Great Britain

Entry flow in a channel. Part 3. Inlet in a uniform stream

By A. K. KAPILA, G. S. S. LUDFORD AND V. O. S. OLUNLOYO

Department of Theoretical and Applied Mechanics, Cornell University, Ithaca, N.Y.

(Received 28 August 1972)

This paper complements earlier papers by Van Dyke (1970) and by Wilson (1971) which have appeared under the same title. Second-order boundary-layer theory is used to examine the region near the entrance to a single channel placed in a uniform stream. It is found that there are additional effects to those present in the three models treated by Van Dyke and Wilson. In particular, the cascade model misses the leading term in the separation force while the irrotational-entry model misses that in the skin friction.

There are also two new effects far downstream: logarithmic terms appear (apparently for the first time in second-order theory); and a resonance with the first eigensolution occurs.

1. Introduction

Although there has been extensive literature, some analytical but most numerical, on the flow in the entrance of a plane channel, it was only two years ago that the problem, in both its aspects, was examined critically from the point of view of boundary-layer theory by Van Dyke (1970). In particular, he showed that previous boundary-layer analysis was valid very far downstream and not at the entrance as had been supposed. A more thorough treatment of the mathematical questions involved in the boundary-layer structure was later given by Wilson (1971).

In numerical work three models are used: (i) infinite cascade, (ii) irrotational entry and (iii) uniform entry. [Van Dyke does not treat (ii) though he acknowledges its significance.] The first of these is quite special while the others are artificial. None of the three can represent actual entry conditions presented by any realistic upstream flow of interest [though Van Dyke speaks of a mesh of varying porosity having been used to produce (iii)]. Such models are used in order to avoid discussing the upstream flow. Indeed Wilson's conclusion that (i) is the most satisfactory and (iii) the least is based on the nature of the second-order boundary layers and not on their simulation of actual upstream flow.

In the present study we examine the flow in a single channel forming an inlet in an otherwise uniform stream (figure 1). While it can be argued that this is the true inlet problem, it suffices to have it recognized as an entry-flow problem incorporating upstream conditions of more interest than those of the cascade.

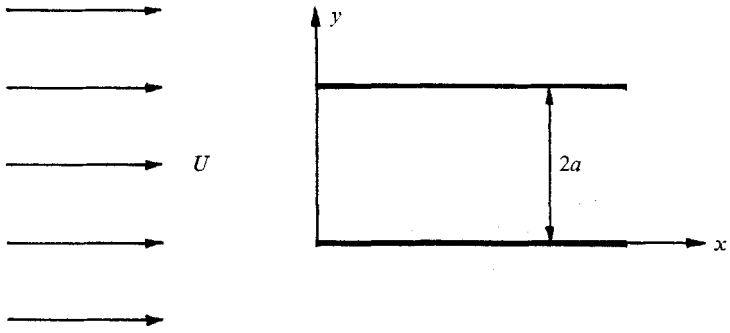

FIGURE 1. Flow geometry.

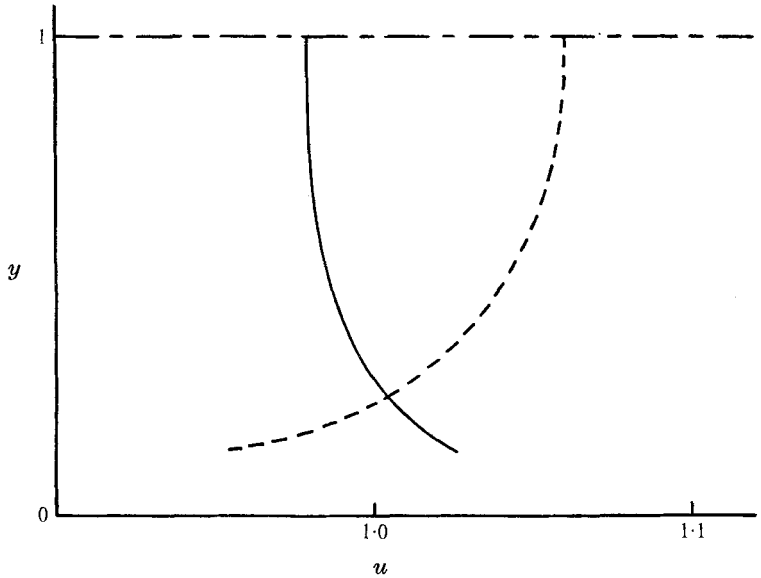

FIGURE 2. Calculated velocity profile across entrance of channel for $R = 75$: – – – –, cascade (Van Dyke 1970); ——, present inlet.

It admits exact solution, in the sense of second-order boundary-layer theory, although the Wiener–Hopf technique is required to derive it (rather than the straightforward Fourier analysis of Van Dyke and Wilson).

As far as a leading edge is concerned, the second-order boundary layer has features which are not present in the cascade but are in the irrotational-entry model (which Wilson considers artificial; in fact, it has a fatal flaw, see §5.1). Neither (i) nor (ii) is completely satisfactory (though the peculiar behaviour for uniform entry is absent)†. The cascade suppresses local circulation, which is the dominant contributor to the forces of separation of the channel walls. Irrotational entry misses the leading skin-friction term.

Far downstream inside the channel the boundary layer is similar to that in the cascade model (discussed by Wilson). However, unlike the cascade (and the other

† The computed streamwise velocity profile across the entrance of the channel is shown in figure 2.

two models) our channel has an outside, the boundary layers on which have a novel feature. As well as the usual inverse powers of the distance x, the inviscid surface speed has such terms multiplied by powers of $x^{-1}\log x$, which induce corresponding terms in the boundary layer. In the classical problem of flow past a semi-infinite flat plate such logarithms only arise in approximations of order higher than the second (Goldstein 1960, chap. 8).

Our set-up exhibits an additional effect, not present in any of the models. If the pressure far downstream inside the channel is not maintained at the correct level, global circulation around each wall of the channel will occur. While nothing new arises in the internal boundary layers, the external boundary layers far downstream exhibit, in addition to logarithmic terms similar to those mentioned above, a resonance. The forcing function associated with the inviscid surface speed contains $x^{-\frac{1}{2}}$, which is also the x dependence of the first eigensolution, resulting in an $x^{-\frac{1}{2}}\log x$ term in the boundary layer. This resonance would in fact occur in the classical problem above if second-order circulation were admitted. Indeed, it even appears at the first order for flow past a parabola (Van Dyke 1964).

While the boundary layer far downstream is only of importance when it comes to matching with the fully diffused regions beyond, the occurrence of these new features is worth noting.

2. Formulation

The half-width a of the channel is chosen as the reference length and the free-stream speed U as the reference velocity. The Reynolds number R is Ua/ν. Then the dimensionless stream function satisfies

$$\left(\psi_y\frac{\partial}{\partial x}-\psi_x\frac{\partial}{\partial y}\right)\nabla^2\psi = R^{-1}\nabla^2(\nabla^2\psi). \tag{2.1}$$

The boundary conditions are those of a uniform flow far upstream and no slip at the walls of the channel, i.e.

$$\psi(x,0)=\psi_y(x,0)=0, \quad \psi\sim y \quad \text{as} \quad x\to-\infty.$$

Owing to the symmetry, the mid-plane of the channel will always be a stream surface, so that

$$\psi(x,1)=1 \quad \text{for all } x$$

and it suffices to consider only the lower half of the configuration ($y\leqslant 1$).

The flow divides itself into an inviscid core and wall boundary layers. In these regions, designated as 'outer' and 'inner' respectively, the stream function may be expanded as

$$\psi\sim\begin{cases}\psi_1(x,y)+R^{-\frac{1}{2}}\psi_2(x,y)+\ldots & \text{in the outer region,}\\ R^{-\frac{1}{2}}\Psi_1(x,Y)+R^{-1}\Psi_2(x,Y)+\ldots & \text{in the inner region,}\end{cases}$$

where $Y=R^{\frac{1}{2}}y$ is the appropriate stretched variable for the inner region. It should be noted that these expansions are valid uniformly only for $x=o(R)$.

An $O(R^{-1})$ region at the leading edge of the wall is also excluded. The first-order solution is just the undisturbed stream $\psi_1 = y$, so that the first-order inner solution is the Blasius boundary layer. Writing $\eta = Y/(2x)^{\frac{1}{2}}$ and $\Psi_1 = (2x)^{\frac{1}{2}} f_0(\pm\eta)$ for $Y \gtrless 0$, we have

$$f_0 = \eta - \beta + \text{a.e.s. in } \eta \text{ for } \eta \text{ large},$$

where a.e.s. stands for terms asymptotically exponentially small and $\beta = 1.21678$.

3. Calculation of the inviscid disturbance

The second-order outer solution ψ_2 is found to satisfy Laplace's equation with boundary conditions

$$\psi_2(x, 1) = 0, \quad \psi_2(x, y) \to 0 \quad \text{as} \quad y \to -\infty \quad \text{for all } x, \tag{3.1}$$

and

$$\psi_{2x}(x, \pm 0) = \pm \tfrac{1}{2} k x^{-\frac{1}{2}} \quad \text{for} \quad x > 0,$$

where $k = -2^{\frac{1}{2}}\beta$. The last equation may be integrated to yield

$$\psi_2(x, \pm 0) = \pm k x^{\frac{1}{2}} + \psi^0 \quad \text{for} \quad x > 0, \tag{3.2}$$

where the integration constant ψ^0 represents a global circulation around the wall. While such a term is easily incorporated in the following analysis, we prefer to deal with it later (§4) and restrict attention here to the flow without global circulation†. Let

$$\psi_2(x, \pm 0) = g(x) \quad \text{for} \quad x < 0 \tag{3.3}$$

and

$$\psi_{2y}(x, +0) - \psi_{2y}(x, -0) = \begin{cases} f(x) & \text{for} \quad x > 0, \\ 0 & \text{for} \quad x < 0, \end{cases} \tag{3.4}$$

where the functions $f(x)$ and $g(x)$ are 'half-unknown', on the positive and the negative x axes respectively.

The Fourier transform is defined as

$$\overline{\psi}(\xi, y) = \int_{-\infty}^{\infty} \psi_2(x, y)\, e^{-i\xi x}\, dx$$

with the inverse

$$\psi_2(x, y) = \frac{1}{2\pi} \int_{-\infty}^{\infty} \overline{\psi}(\xi, y)\, e^{i\xi x} d\xi.$$

On occasion, it may be necessary to indent the contour of integration above or below the origin in the complex ξ plane.

The Fourier transform of Laplace's equation has the solution

$$\overline{\psi}(\xi, y) = \begin{cases} (\bar{g}_+ + \bar{n}_-) \dfrac{\sinh\{|\xi|(1-y)\}}{\sinh|\xi|} & \text{for} \quad 0 < y \leqslant 1, \\ (\bar{g}_+ - \bar{n}_-)\, e^{|\xi| y} & \text{for} \quad -\infty < y < 0 \end{cases} \tag{3.5}$$

† A referee has suggested that the conformal mapping used in §4 may secure the results more quickly than the Wiener–Hopf technique adopted here. However, we were unable to complete the asymptotics that way, while non-trivial modifications of standard Wiener–Hopf arguments (§3 and appendix) did yield them.

satisfying the boundary conditions (3.1)–(3.3). Here†

$$\bar{n}_- = k\sqrt{\pi}/2(i\xi)^{\frac{3}{2}} \tag{3.6}$$

corresponding to $$n(x) = \begin{cases} 0 & \text{for} \quad x < 0, \\ kx^{\frac{1}{2}} & \text{for} \quad x > 0. \end{cases}$$

Similarly the 'half-unknown' functions $f(x)$ and $g(x)$ transform into $\bar{f}_-(\xi)$ and $\bar{g}_+(\xi)$ respectively. In the usual way we write

$$|\xi| = (\xi + i\epsilon)^{\frac{1}{2}}(\xi - i\epsilon)^{\frac{1}{2}}$$

and take the limit $\epsilon \to 0$ at the end. The jump condition (3.4) now leads to the Wiener–Hopf equation

$$\bar{g}_+ K + \bar{n}_-|\xi|(\coth|\xi| - 1) = -\bar{f}_-,$$

where $$K(\xi) = \xi e^{|\xi|}/\sinh\xi.$$

The overlap strip of regularity is $-\epsilon < \operatorname{Im}\xi < 0$.

It is possible to factorize the kernel:

$$K(\xi) = K_+(\xi)\,K_-(\xi),$$

where the $K_\pm$ are two zeroless functions with algebraic growth as $\xi \to \infty$ in the appropriate half-planes. Details of the $K_\pm$ are given in the appendix. The Wiener–Hopf equation may then be written as

$$\bar{g}_+ K_+ + P = -\bar{f}_-/K_-, \tag{3.7}$$

where $$P(\xi) = (\bar{n}_-/K_-)\,|\xi|\,(\coth|\xi| - 1)$$

is regular in the overlap strip and decays (exponentially) as $\operatorname{Re}\xi \to \pm\infty$. It can therefore be decomposed as the sum $P_+ + P_-$, with

$$P_+(\xi) = \frac{1}{2\pi i}\int_{C_-} \frac{\bar{n}_-|z|\,(\coth|z| - 1)}{K_-(z - \xi)}\,dz \quad \text{for Im } \xi > 0, \tag{3.8}$$

where the path of integration C_- is from $-\infty$ to ∞ and is indented below the point $z = 0$. A similar expression holds for P_-. Details of P_+ are given in the appendix. If now (3.7) is written as

$$\bar{g}_+ K_+ + P_+ = -P_- - \bar{f}_-/K_-,$$

the left-hand side is regular in the upper half-plane $\operatorname{Im}\xi > -\epsilon$ and the right-hand side is regular in the overlapping lower half-plane $\operatorname{Im}\xi < 0$. Together the two sides of the equation define an entire function which must be zero if the force of separation of the channel walls is to be integrable at the leading edge. Thus

$$\bar{g}_+ = -P_+/K_+. \tag{3.9}$$

Substitution of $\bar{g}_+$ into (3.5) now gives the stream function. (Details of $\bar{g}_+$ are given in the appendix.)

Of greater interest, however, is the displacement speed $\psi_{2y}(x, \pm 0)$, because it provides the matching condition for the second-order boundary layer and is

† The subscripts + or − indicate whether a function is regular in the upper or the lower half-planes as defined by the strip of regularity below.

also the negative of the disturbance pressure. It is not possible to obtain a closed-form expression for $\psi_{2y}(x, \pm 0)$, but its behaviour along different stretches of the x axis can be ascertained.

3.1. *Displacement speed near the leading edge*

To determine $\psi_{2y}(x, \pm 0)$ near the leading edge of the wall it is best to look at its Fourier transform

$$\overline{\psi}(\xi, \pm 0) = \begin{cases} -(\bar{g}_+ + \bar{n}_-)|\xi| \coth|\xi|, \\ (\bar{g}_+ - \bar{n}_-)|\xi|. \end{cases} \tag{3.10}$$

The transform must be decomposed into functions regular in half-planes. The asymptotic expansions of these functions for large ξ then give the required behaviour. For convenience, we write

$$F_1 = \bar{n}_-|\xi|(\coth|\xi| - 1),$$
$$F_2 = \bar{g}_+|\xi|(\coth|\xi| - 1), \quad F_3 = \bar{n}_-|\xi|, \quad F_4 = \bar{g}_+|\xi|,$$

and treat each in turn.

(i) We have

$$F_{1-}(\xi) = -\frac{1}{2\pi i}\int_{C_-} \frac{\bar{n}_-|z|(\coth|z| - 1)}{z - \xi} dz \text{ for } \operatorname{Im}\xi < 0.$$

Because of the exponential convergence provided by $(\coth|z| - 1)$, F_{1-} can be expanded for large ξ by writing

$$\frac{1}{z - \xi} = -\frac{1}{\xi}\left(1 + \frac{z}{\xi} + \ldots\right)$$

and integrating term by term. Thus

$$F_{1-} \sim k\left\{\frac{a_1}{i\xi} + \frac{a_2}{(i\xi)^2} + \ldots\right\},$$

where

$$a_n = \frac{i^{n-\frac{5}{2}}}{4\sqrt{\pi}}\int_{C_-} \frac{|z|(\coth|z| - 1)z^{n-1}}{z^{\frac{3}{2}}} dz. \tag{3.11}$$

The integration may be taken along the real axis for every n except $n = 1$, in which case the $z^{-\frac{3}{2}}$ singularity at the origin must first be subtracted out. The a_n are all real.†

(ii) The expansion of

$$F_{2-}(\xi) = -\frac{1}{2\pi i}\int_{-\infty}^{\infty} \frac{\bar{g}_+|z|(\coth|z| - 1)}{z - \xi} dz$$

for large ξ is obtained in the same way and the result is

$$F_{2-} \sim k\left\{\frac{c_1}{i\xi} + \frac{c_2}{(i\xi)^2} + \ldots\right\},$$

where

$$c_n = \frac{i^{n-1}}{2\pi k}\int_{-\infty}^{\infty} \bar{g}_+|z|(\coth|z| - 1)z^{n-1} dz. \tag{3.12}$$

† The first few a_n and other coefficients appearing later are listed in tables 1, 2 and 3.

n	a_n	b_n	d_n
1	0·730	−0·380	−0·417
2	0·326	0·252	−0·180
3	0·126	−0·268	−0·059

TABLE 1

n	A_n	C_n	e_n
0	−1·000	0·141	−0·399
1	−0·083	0·0	−0·333
2	−0·028	1·738	−0·208

TABLE 2

m	n	l_{mn}	D_{mn}
0	0	0·318	−2·367
0	1	−0·683	−2·375
1	1	−0·318	4·734

TABLE 3

The integration may be taken along the real axis for all n; the c_n are all real and independent of k.

(iii) The integral

$$F_{3-}(\xi) = -\frac{1}{2\pi i}\int_{-\infty}^{\infty} \frac{\bar{n}_-|z|}{z-\xi}\,dz$$

can be evaluated explicitly by writing

$$z^{\frac{3}{2}} = \lim_{\epsilon\to 0}(z-i\epsilon)^{\frac{3}{2}}.$$

By completing the contour in the upper half-plane we find that the integral is of $O(\epsilon^{\frac{1}{2}})$, so that in the limit $F_{3-} = 0$.

(iv) To deal with

$$F_{4-}(\xi) = -\frac{1}{2\pi i}\int_{C_+} \frac{\bar{g}_+|z|}{z-\xi}\,dz,$$

where the path of integration C_+ is from $-\infty$ to ∞ and is indented above the point $z = 0$, we subtract out from $\bar{g}_+$ the leading term of its asymptotic expansion for large z (see the appendix) so that

$$F_{4-} = -\frac{kb_1}{2\pi i}\int_{C_+} \frac{|z|\,dz}{(-iz)^{\frac{3}{2}}(z-\xi)} - \frac{1}{2\pi i}\int_{C_+} \frac{|z|\,\{\bar{g}_+ - kb_1/(-iz)^{\frac{3}{2}}\}}{z-\xi}\,dz.$$

By expressing $z^{\frac{3}{2}}$ [which now has the cut $(-i\infty, 0)$] as

$$\lim_{\epsilon\to 0}(z+i\epsilon)^{\frac{3}{2}}$$

and then completing the contour in the lower half-plane, the first integral may be explicitly evaluated as a multiple of $\xi^{-\frac{1}{2}}$. We now rewrite the second integral to get

$$F_{4-} = -\frac{kb_1}{(i\xi)^{\frac{1}{2}}} + \frac{kd_1}{i\xi} - \frac{1}{2\pi i\xi}\int_{C_+} \frac{|z|\{\bar{g}_+ - kb_1/(-iz)^{\frac{3}{2}}\}z}{z-\xi}\,dz,$$

where $$d_1 = \frac{1}{2\pi k}\int_{C_+} |z|\left\{\bar{g}_+ - \frac{kb_1}{(-iz)^{\frac{3}{2}}}\right\}dz.$$

The leading pair of terms in the expansion of F_{4-} is thus determined. To get higher pairs, we subtract out from $\bar{g}_+$ more terms in its expansion for large z. The result is

$$F_{4-} \sim k\left\{-\frac{b_1}{(i\xi)^{\frac{1}{2}}} + \frac{d_1}{i\xi} + \frac{b_2}{(i\xi)^{\frac{3}{2}}} + \frac{d_2}{(i\xi)^2} - \frac{b_3}{(i\xi)^{\frac{5}{2}}} + \ldots\right\},$$

where the b_n are defined in the appendix and

$$d_n = \frac{(i)^{n-1}}{2\pi k} C_+ \int_{-\infty}^{\infty} |z|\left\{\bar{g}_+ - \frac{kb_1}{(-iz)^{\frac{3}{2}}} - \ldots - \frac{kb_n}{(-iz)^{n+\frac{1}{2}}}\right\} z^{n-1}\,dz. \tag{3.13}$$

The coefficients d_n are all real and independent of k.

In a similar manner, the expansions for the + parts of the F's can be determined:

$$F_{1+} \sim -k\left\{\frac{a_1}{i\xi} + \frac{a_2}{(i\xi)^2} + \ldots\right\},$$

$$F_{2+} \sim -k\left\{\frac{c_1}{i\xi} + \frac{c_2}{(i\xi)^2} + \ldots\right\},$$

$$F_{3+} = -k\sqrt{\pi}/2(-i\xi)^{\frac{1}{2}},$$

$$F_{4+} \sim -k\left\{\frac{d_1}{i\xi} + \frac{d_2}{(i\xi)^2} + \ldots\right\}.$$

Now, in terms of the F's, equation (3.10) can be written as

$$\bar{\psi}_y(\xi, \pm 0) = \begin{cases} -(F_1 + F_2 + F_3 + F_4), \\ -F_3 + F_4, \end{cases}$$

so that

$$\bar{\psi}_{y-}(\xi, +0) \sim -k\left\{-\frac{b_1}{(i\xi)^{\frac{1}{2}}} + \frac{a_1 + c_1 + d_1}{i\xi} + \frac{b_2}{(i\xi)^{\frac{3}{2}}} + \frac{a_2 + c_2 + d_2}{(i\xi)^2} - \ldots\right\},$$

$$\bar{\psi}_{y-}(\xi, -0) \sim k\left\{\frac{-b_1}{(i\xi)^{\frac{1}{2}}} + \frac{d_1}{i\xi} + \frac{b_2}{(i\xi)^{\frac{3}{2}}} + \frac{d_2}{i\xi} - \ldots\right\},$$

$$\bar{\psi}_{y+}(\xi, +0) \sim \frac{k\sqrt{\pi}}{2(-i\xi)^{\frac{1}{2}}} + k\left\{\frac{a_1 + c_1 + d_1}{i\xi} + \frac{a_2 + c_2 + d_2}{(i\xi)^2} + \ldots\right\},$$

$$\bar{\psi}_{y+}(\xi, -0) \sim \frac{k\sqrt{\pi}}{2(-i\xi)^{\frac{1}{2}}} - k\left\{\frac{d_1}{i\xi} + \frac{d_2}{(i\xi)^2} + \ldots\right\}.$$

Since the displacement speed is continuous across the negative x axis,

$$\bar{\psi}_{y+}(\xi, +0) = \bar{\psi}_{y+}(\xi, -0)$$

and therefore $$a_n + c_n + d_n = -d_n. \tag{3.14}$$

We were unable to prove this result directly without introducing the + functions. They would not otherwise have been introduced since the behaviour of ψ_{2y} as $x \to 0-$ is not of great interest.

Fourier inversion and the use of (3.14) now yield

$$\psi_{2y}(x, \pm 0) \sim k\left\{ \pm \frac{b_1}{\Gamma(\frac{1}{2})} x^{-\frac{1}{2}} + d_1 \mp \frac{b_2}{\Gamma(\frac{3}{2})} x^{\frac{1}{2}} + \frac{d_2}{\Gamma(2)} x \pm \frac{b_3}{\Gamma(\frac{5}{2})} x^{\frac{3}{2}} + \ldots \right\} \quad \text{as} \quad x \to 0+. \tag{3.15}$$

We now direct attention to this last result (which holds, of course, outside an $O(R^{-1})$ neighbourhood of the leading edge). A comparison with Wilson's results shows that neither the cascade nor the irrotational-entry version of the inlet problem correctly describes the flow near the leading edge. The cascade model misses the $O(x^{-\frac{1}{2}})$ term, which provides the major contribution to the forces of separation between the channel walls, as well as all following half-powers; whereas the irrotational-entry model suppresses the $O(1)$ term, which is the dominant contributor to leading-edge skin friction, and all following half-powers.

The $O(x^{-\frac{1}{2}})$ term in the inviscid surface speed represents a local circulation around the leading edge. Wilson encounters this term only for irrotational entry and contends that it 'reflects the artificial imposition of a boundary condition at the inlet'. However, as pointed out by Ludford & Olunloyo (1972*a*), leading-edge circulation is a genuine characteristic of flows that are not symmetrically bounded. Indeed, on writing (3.15) in a dimensional form and letting the channel half-width $a \to \infty$ it can be seen that the $O(x^{-\frac{1}{2}})$ term survives in the limit, i.e. the asymmetry of the flow is preserved however far apart the two walls of the channel are. It is the forced symmetry imposed by the cascade that suppresses the local circulation.

3.2. *Displacement speed far downstream*

The behaviour of $\psi_{2y}(x, \pm 0)$ far downstream is determined by expanding the transform $\overline{\psi}_y(\xi, \pm 0)$ near its lowest singularity (the origin) in the upper half-plane. From (3.10), we get

$$\overline{\psi}_y(\xi, +0) = -\bar{g}_+ \xi \coth \xi - k\sqrt{\pi} \sum_{p=0}^{n} \frac{(-1)^p 2^{2p-1} \bar{B}_{2p}}{(2p)!} (i\xi)^{2p-\frac{3}{2}} + O(\xi^{2n+\frac{1}{2}}), \tag{3.16}$$

where the $\bar{B}_{2p}$ are the Bernoulli numbers, and

$$\overline{\psi}_y(\xi, -0) = -\frac{k\sqrt{\pi}}{2(i\xi)^{\frac{3}{2}}} |\xi| - \tfrac{1}{2}k \sum_{p=0}^{n} \left[\tilde{A}_p |\xi| (-i\xi)^{p-\frac{1}{2}} + |\xi| (-i\xi)^p \sum_{r=0}^{p} \tilde{B}_{rp} \{\log(-i\xi)\}^r \right] + O(\xi^{n+\frac{3}{2}}), \tag{3.17}$$

where (A 10) (from the appendix) has been used. Upon Fourier inversion, the first term of (3.16) contributes an exponentially small term, since its lowest singularity is at $\xi = i\pi$ and not at $\xi = 0$; while the remainder yield

$$\psi_{2y}(x, +0) = k \sum_{p=0}^{n} \frac{A_p}{x^{2p-\frac{1}{2}}} + O(x^{-2n-\frac{1}{2}}) \quad \text{as} \quad x \to +\infty, \tag{3.18}$$

where

$$A_p = (-1)^p \frac{2^{2p-1} \bar{B}_{2p} \Gamma(2p - \frac{1}{2})}{(2p)! \sqrt{\pi}}. \tag{3.19}$$

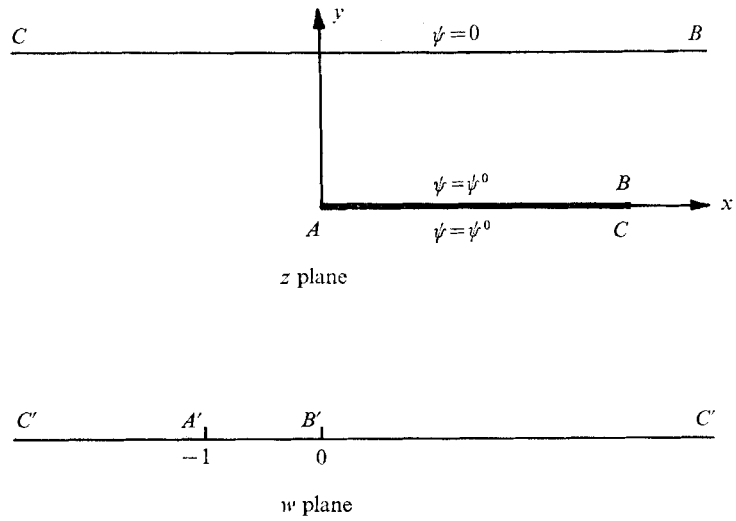

FIGURE 3. Mapping lower half of flow region in z plane onto upper half of w plane.

In (3.17) the contribution from the first term vanishes in the limit $\epsilon \to 0$ and the remainder yield

$$\psi_{2y}(x, -0) = k \sum_{p=0}^{n} \left[C_p x^{-p-\frac{3}{2}} + x^{-p-2} \sum_{r=0}^{p} D_{rp} (\log x)^r \right] + O(x^{-n-\frac{5}{2}}) \quad \text{as} \quad x \to +\infty, \tag{3.20}$$

where

$$C_p = (2\pi)^{-1} \tilde{A}_p \, \Gamma(p + \tfrac{3}{2}) \tag{3.21}$$

and the D_{rp} are related to the $\tilde{B}_{rp}$ by the expression

$$x^{-p-2} \sum_{r=0}^{p} D_{rp} (\log x)^r = \frac{1}{2\pi} \sum_{r=0}^{p} \tilde{B}_{rp} \frac{\partial^r}{\partial p^r} \{x^{-p-2} \, \Gamma(p+2)\}. \tag{3.22}$$

These results indicate that inside the channel the inviscid speed increases like $x^{\frac{1}{2}}$ far downstream. This acceleration in the core is caused by the thickening boundary layers at the walls. Outside the channel, the inviscid speed decays like $x^{-\frac{3}{2}}$.

4. Global circulation

Global circulation around the channel wall has been avoided by omitting the integration constant in condition (3.2). Although the Wiener–Hopf analysis can be modified to take account of this constant, conformal mapping gives the results more easily.

The transformation

$$z = -\pi^{-1}(w + \log w + 1) + i$$

maps the half-plane $\operatorname{Im} z < 1$ slit along the positive real axis onto the upper half of the w plane as shown in figure 3. The circulation solution is therefore

$$\psi^c = \pi^{-1} \psi^0 \operatorname{Im} (\log w),$$

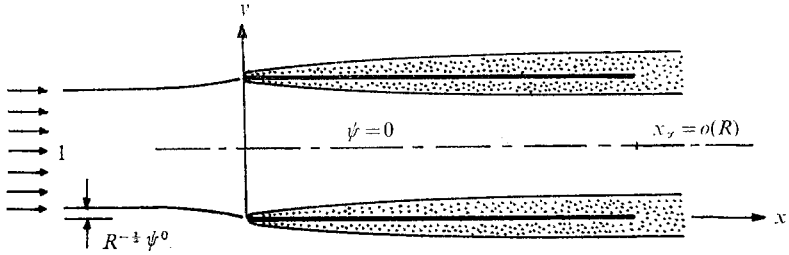

FIGURE 4. Application to finite channel, terminating well before the interior boundary layers join.

ψ^0 being the constant value of the stream function on the wall. The corresponding x velocity is

$$\psi^c_y(x, y) = -\psi^0 \operatorname{Re}(w+1)^{-1}.$$

The leading edge maps into $w = -1$ and expansion near it gives

$$\psi^c_y(x, \pm 0) \sim \psi^0 \sum_{p=0}^{\infty} (\pm 1)^{p-1} e_p x^{\frac{1}{2}(p-1)} \quad \text{as} \quad x \to 0+, \tag{4.1}$$

where the e_p are given by the relation

$$\left\{\sum_{p=0}^{\infty} e_p z^{\frac{1}{2}(p-1)}\right\}^{-1} - \log\left[1 + \left\{\sum_{p=0}^{\infty} e_p z^{\frac{1}{2}(p-1)}\right\}^{-1}\right] = \pi z. \tag{4.2}$$

Infinity downstream inside and outside the channel map into $w = 0_-$ and $w = -\infty$ respectively. Expansions there yield

$$\psi^c_y(x, \pm 0) \sim \left\{\begin{array}{c} -\psi_0 + \text{a.e.s. in } x \\ \psi_0 \sum\limits_{p=0}^{\infty} x^{-p-1} \sum\limits_{r=0}^{\infty} l_{rp} (\log x)^r \end{array}\right\} \quad \text{as} \quad x \to +\infty, \tag{4.3}$$

where the l_{rp} are given by the relation

$$\left\{\sum_{p=0}^{\infty} z^{-p-1} \sum_{r=0}^{\infty} l_{rp} (\log z)^r\right\}^{-1} - \log\left[1 + \left\{\sum_{p=0}^{\infty} z^{-p-1} \sum_{r=0}^{\infty} (\log z)^r\right\}^{-1}\right] = \pi z. \tag{4.4}$$

The value of ψ^0 is fixed by downstream conditions in the channel. For example, if the channel is terminated at $x = x_\infty \gg 1$ (see figure 4), the resultant equalization of pressure inside and outside at that section makes

$$\psi^0 = k A_0 x_\infty^{\frac{1}{2}} \text{ approximately.}$$

Here (3.18), (3.20) and (4.3) have been used.

5. Second-order boundary layer

In this section, the second-order stream function Ψ_2 is examined. Writing $\Psi_2(x, Y) = g(x, \eta)$ and inserting the inner expansion

$$\psi \sim R^{-\frac{1}{2}}\Psi_1 + R^{-1}\Psi_2 + \ldots$$

into the full Navier–Stokes equation (2.1), g is found to satisfy

$$g_{\eta\eta\eta\eta} + f_0 g_{\eta\eta\eta} + 2f_0' g_{\eta\eta} + f_0'' g_\eta + 2x(f_0''' g_x - f_0' g_{\eta\eta x}) = 0,$$

f_0 being the Blasius function. The boundary conditions are

$$g(x,0) = g_\eta(x,0) = 0, \quad g_\eta = F(x) + \text{a.e.s. in } \eta \quad \text{as} \quad \eta \to \infty,$$

where the forcing function

$$F(x) = (2x)^{\frac{1}{2}} \psi_{2y}(x, \pm 0). \tag{5.1}$$

5.1. *Expansion near the leading edge*

From (3.15) and (5.1), the asymptotic expansion of $F(x)$ as $x \to 0+$ is

$$F(x) \sim \sqrt{2^{\frac{1}{2}}k} \sum_{p=0}^{\infty} \left\{ \pm(-1)^p \frac{b_{p+1}}{\Gamma(p+\frac{1}{2})} x^p + \frac{d_{p+1}}{\Gamma(p+1)} x^{p+\frac{1}{2}} \right\} \quad \text{for} \quad y = \pm 0.$$

This suggests the boundary-layer expansion

$$g \sim 2^{\frac{1}{2}}k \sum_{p=0}^{\infty} \left\{ \pm(-1)^p \frac{b_{p+1}}{\Gamma(p+\frac{1}{2})} x^p G_p(\eta) + \frac{d_{p+1}}{\Gamma(p+1)} x^{p+\frac{1}{2}} G_{p+\frac{1}{2}}(\eta) \right\}$$
$$\text{as} \quad x \to 0+ \quad \text{for} \quad y = \pm 0, \tag{5.2}$$

where the G_λ, for all real λ, satisfy

$$L_\lambda[G_\lambda] \equiv \frac{d}{d\eta}\left\{\frac{d^3}{d\eta^3} + f_0 \frac{d^2}{d\eta^2} + (1-2\lambda) f_0' \frac{d}{d\eta} + 2\lambda f_0''\right\} G_\lambda = 0$$

subject to the conditions

$$G_\lambda(0) = G_\lambda'(0) = 0, \quad G_\lambda' = 1 + \text{a.e.s. in } \eta \quad \text{as} \quad \eta \to \infty.$$

The second-order dimensionless shear at the wall is

$$C_f = 2R^{-1}\Psi_{2yy}(x, \pm 0)$$
$$= R^{-1} \sum_{p=0}^{\infty} \left\{ \pm(-1)^p \frac{b_{p+1}}{\Gamma(p+\frac{1}{2})} G_p''(0)\, x^{p-1} + \frac{d_{p+1}}{\Gamma(p+1)} G_{p+\frac{1}{2}}''(0)\, x^{p-\frac{1}{2}} \right\}. \tag{5.3}$$

When the two sides of the wall are considered jointly, only the fractional powers of x survive in (5.3), the integral powers cancelling.

Wilson, who considers only one side of the wall in his irrotational-entry analysis, observes that the non-integrable $O(x^{-1})$ term in the shear stress is absent because its multiplying factor $G_0''(0)$ [$h''_{-\frac{1}{2}}(0)$ in his notation] is zero. That this is not so has been shown by Ludford & Olunloyo (1972*b*), who obtain a result equivalent to $G_0''(0) = -\beta$. They also point out that the presence of non-integrable leading-edge skin friction raises a doubt about the physical realism of the irrotational model, in which only the inside of the channel is considered.

The values of $G''_{\frac{1}{2}(p+1)}(0)$ for $p = 0, 1, \ldots, 5$ have been given (correctly) by Wilson [his $g_n''(0)$ for $n = 0, 1, \ldots, 5$]. There is little interest in the $G_p''(0)$ since they disappear from the two-sided shear result, as noted above.

5.2. *Expansion far downstream*

For $y = +0$, $F(x)$ has the expansion

$$F(x) \sim 2^{\frac{1}{2}}k \sum_{p=0}^{\infty} A_p x^{-2p+1} \quad \text{as} \quad x \to +\infty,$$

where the A_p are defined by (3.19). Consequently, the boundary-layer expansion may be written as

$$g \sim 2^{\frac{1}{2}}k\left\{\sum_{p=0}^{\infty} A_p x^{-2p+1} G_{-2p+1}(\eta) + \sum_{\gamma} \bar{A}_\gamma x^\gamma \bar{G}_\gamma(\eta)\right\} \quad \text{as} \quad x \to +\infty. \tag{5.4}$$

Here, the first set of terms is the result of direct matching with the expansion for $F(x)$, while the second set consists of the eigensolutions. The γ are the eigenvalues and the $\bar{G}_\gamma$ the corresponding eigenfunctions of the homogeneous problem, i.e.

$$L_\gamma[\bar{G}_\gamma] = 0, \quad \bar{G}_\gamma(0) = \bar{G}'_\gamma(0) = 0, \quad \bar{G}'_\gamma = \text{a.e.s. in } \eta \quad \text{as} \quad \eta \to \infty.$$

Libby & Fox (1963) have shown that the eigenvalues are all real and negative and form a countable set, the first few being $-\frac{1}{2}$, $-1{\cdot}387$, $-2{\cdot}314, \ldots$. The coefficients $\bar{A}_\gamma$ cannot be determined by direct matching; indeed Wilson has shown how they depend upon the global character of $F(x)$.

Thus, far downstream inside the channel the leading term in the boundary-layer expansion is of $O(x)$, followed by the $O(x^{-\frac{1}{2}})$ eigensolution and then by the $O(x^{-1})$ forced term, as predicted by Wilson in his cascade analysis.

For $y = -0$,

$$F(x) \sim 2^{\frac{1}{2}}k\left[\sum_{p=0}^{\infty} C_p x^{-p-1} + \sum_{p=0}^{\infty} x^{-p-\frac{3}{2}} \sum_{r=0}^{p} D_{rp} (\log x)^r\right] \quad \text{as} \quad x \to +\infty,$$

where the coefficients C_p and D_{rp} are defined by (3.21) and (3.22) respectively. The boundary-layer expansion may then be written as

$$g \sim 2^{\frac{1}{2}}k\left[\sum_{p=0}^{\infty} C_p x^{-p-1} G_{-p-1}(\eta) + \sum_{p=0}^{\infty} x^{-p-\frac{3}{2}} \sum_{r=0}^{p} (\log x)^r G^r_{-p-\frac{3}{2}}(\eta) + \sum_{\gamma} \bar{C}_p x^\gamma \bar{G}_\gamma(\eta)\right]$$
$$\text{as} \quad x \to +\infty. \tag{5.5}$$

Here, the $G^r_{-p-\frac{3}{2}}$ satisfy

$$L_{-p-\frac{3}{2}}[G^r_{-p-\frac{3}{2}}] = 2(r+1)\{f'_0 G''^{r+1}_{-p-\frac{3}{2}} - f'''_0 G^{r+1}_{-p-\frac{3}{2}}\}$$

for $r = 0, 1, \ldots, (p-1)$, and

$$L_{-p-\frac{3}{2}}[G^p_{-p-\frac{3}{2}}] = 0$$

subject to the conditions

$$G^r_{-p-\frac{3}{2}}(0) = G'^r_{-p-\frac{3}{2}}(0) = 0, \quad G'^r_{-p-\frac{3}{2}} = D_{rp} + \text{a.e.s. in } \eta \quad \text{as} \quad \eta \to \infty.$$

The last set of terms in (5.5) again consists of the eigensolutions, the coefficients $\bar{C}_p$ being indeterminate as regards matching. Thus, outside the channel, the dominant term at infinity is the $O(x^{-\frac{1}{2}})$ eigensolution, followed by the $O(x^{-1})$ forced term.

5.3. *Global-circulation boundary layer*

Near the leading edge and far downstream inside the channel, the expansions for the circulation boundary-layer stream function $g^c(x, \eta)$ can be determined by straightforward matching with the corresponding expansions of the forcing function $F^c(x) = (2x)^{\frac{1}{2}} \psi^c_y(x, \pm 0)$. The results are

$$g^c \sim 2^{\frac{1}{2}}\psi^0 \begin{cases} \displaystyle\sum_{p=0}^{\infty} (\pm 1)^{p-1} e_p x^{\frac{1}{2}p} G_{\frac{1}{2}p}(\eta) & \text{as} \quad x \to 0+, \\ \displaystyle -x^{\frac{1}{2}} G_{\frac{1}{2}}(\eta) + \sum_{\gamma} \bar{M}_\gamma x^\gamma \bar{G}_\gamma(\eta) & \text{as} \quad x \to +\infty. \end{cases} \tag{5.6}$$

Here $\bar{M}_\gamma$ are the indeterminate multipliers of the eigenfunctions $\bar{G}_\gamma$. In obtaining (5.6), (4.2) and (4.3) have been used.

Far downstream outside the channel the boundary-layer expansion exhibits a resonance which will be described in some detail. From (4.3),

$$F^c(x) \sim 2^{\frac{1}{2}} \psi^0 \sum_{p=0}^{\infty} x^{-p-\frac{1}{2}} \sum_{r=0}^{p} l_{rp} (\log x)^r \quad \text{as} \quad x \to +\infty.$$

The exponent $-\frac{1}{2}$ of the leading term in this expansion coincides with the first eigenvalue†, so that the corresponding term in the boundary-layer expansion is taken to be $2^{\frac{1}{2}} \psi^0 l_{00} x^{-\frac{1}{2}} [G(\eta) + \log x H(\eta)]$, where

$$L_{-\frac{1}{2}}[H] = 0, \quad H(0) = H'(0) = 0, \quad H' = \text{a.e.s.in } \eta \quad \text{as} \quad \eta \to \infty \tag{5.7}$$

and

$$L_{-\frac{1}{2}}[G] = 2(f_0' H'' - f_0''' H), \quad G(0) = G'(0) = 0,$$

$$G' = 1 + \text{a.e.s. in } \eta \quad \text{as} \quad \eta \to \infty. \tag{5.8}$$

The general solution of (5.7) is a multiple of the first eigensolution $\bar{G}_{-\frac{1}{2}}$, the latter being known explicitly. Thus,

$$H = \hat{C} \bar{G}_{-\frac{1}{2}} = \hat{C}(\eta f_0' - f_0), \tag{5.9}$$

where $\hat{C}$ is a constant which must be determined such that the problem (5.8) possesses a solution. To find the value of $\hat{C}$ we integrate the differential equation (5.8) once, using (5.9), to get

$$\left\{ \frac{d^3}{d\eta^3} + f_0 \frac{d^2}{d\eta^2} + 2f_0' \frac{d}{d\eta} - f_0'' \right\} G = 2(1 - \hat{C} f_0''').$$

The problem of determining $\hat{C}$ so that this equation possesses a solution satisfying the boundary conditions in (5.8) has been considered by Wilson in a different context [see Wilson 1971, p. 793, reading G, f_0 and $-\hat{C}$ for his h_0, f_1 and k]. We need not repeat his arguments here, but only quote his result $\hat{C} = -1{\cdot}70$. If $\hat{G}$ is a particular solution of equation (5.8) for this value of $\hat{C}$, the general solution is $\hat{G} + \bar{l}_{-\frac{1}{2}} (\eta f_0' - f_0)$, $\bar{l}_{-\frac{1}{2}}$ being an arbitrary constant not determined by matching. The boundary-layer expansion can now be written as

$$g^c \sim 2^{\frac{1}{2}} \psi^0 \Bigg[l_{00} x^{-\frac{1}{2}} \{\hat{G}(\eta) + \bar{l}_{-\frac{1}{2}} (\eta f_0' - f_0)\} - 1{\cdot}70 x^{-\frac{1}{2}} \log x (\eta f_0' - f_0) + \sum_{p=1}^{\infty} x^{-p-\frac{1}{2}} \sum_{r=0}^{p} (\log x)^r G^r_{-p-\frac{1}{2}}(\eta) + \sum_{\substack{\gamma \\ (\gamma \neq -\frac{1}{2})}} x^\gamma \bar{l}_\gamma \bar{G}_\gamma(\eta) \Bigg]. \tag{5.10}$$

Here, the $G^r_{-p-\frac{1}{2}}$ satisfy

$$L_{-p-\frac{1}{2}}[G^r_{-p-\frac{1}{2}}] = 2(r+1)\{f_0' G''^{r+1}_{-p-\frac{1}{2}} - f_0''' G^{r+1}_{-p-\frac{1}{2}}\}$$

for $r = 0, 1, \ldots (p-1)$, and

$$L_{-p-\frac{1}{2}}[G^p_{-p-\frac{1}{2}}] = 0$$

† A similar term arises in the first-order boundary layer on a parabola. In fact, in that context Van Dyke (1964) calculated the equivalent of $\hat{C}$ below in the same way as Wilson did later.

subject to the conditions

$$G^r_{-p-\frac{1}{2}}(0) = G'^r_{-p-\frac{1}{2}}(0) = 0, \quad G'^r_{-p-\frac{1}{2}} = l_{rp} + \text{a.e.s. in } \eta \quad \text{as} \quad \eta \to \infty.$$

The multipliers $\bar{l}_\gamma$ of the eigensolutions $\bar{G}_\gamma$ are indeterminate again, as regards matching.

This research was supported partly by the U.S. Army Research Office, Durham and partly by the National Science Foundation under Grant GP-28483.

Appendix. Details of $K_\pm$, P_+ and $\bar{g}_+$

The factors of $K(z)$ are given by

$$K_\pm(z) = \Gamma\left(1 \mp i\frac{z}{\pi}\right) \exp\left[\frac{1}{\pi}(z^2+\epsilon^2)^{\frac{1}{2}}\left(\frac{\pi}{2} \pm i \log\frac{z+(z^2+\epsilon^2)^{\frac{1}{2}}}{\epsilon}\right) \mp i\frac{z}{\pi}\left(1-\log\frac{\epsilon}{2\pi}\right)\right]. \tag{A 1}$$

The branch cut for $K_\pm$ extends from $\mp i\epsilon$ to $\mp i\infty$, the branch of the logarithm being chosen so that $\frac{1}{2}\pi \pm i \log\{[z+(z^2+\epsilon^2)^{\frac{1}{2}}]/\epsilon\}$ vanishes at $\pm i\epsilon$.

For large z,

$$K_\pm \sim (\mp 2iz)^{\frac{1}{2}}\left\{1 + \frac{\alpha_1}{z}(\pm i\pi) + \frac{\alpha_2}{z^2}(\pm i\pi)^2 + \ldots\right\} \quad \text{for} \quad \epsilon = 0, \tag{A 2}$$

where the coefficients α_n are the same as those in Stirling's formula

$$\Gamma(z) \sim (2\pi)^{\frac{1}{2}} \exp\{-z + (z-\tfrac{1}{2})\log z\}\left\{1 + \frac{\alpha_1}{z} + \frac{\alpha_2}{z^2} + \ldots\right\}.$$

For small z,

$$K_\pm^{-1}(\pi z) \sim 1 \mp iz[\beta_0 \log(\mp iz) + \beta_1] + (\mp iz)^2\left[\frac{1}{2!}\beta_0\{\log(\mp iz)\}^2 + \beta_1 \log(\mp iz) + \beta_2\right] + \ldots \quad \text{for} \quad \epsilon = 0, \tag{A 3}$$

where

$$\beta_0 = 1, \quad \beta_n = \tilde{\alpha}_n - \tilde{\alpha}_{n-1} + \frac{1}{2!}\tilde{\alpha}_{n-2} - \ldots + (-1)^{n-1}\frac{1}{(n-1)!}\tilde{\alpha}_1 + (-1)^n\frac{1}{n!}, \tag{A 4}$$

$\tilde{\alpha}_n$ being the coefficients in the expansion

$$[\Gamma(1+z)]^{-1} = 1 + \sum_{n=1}^{\infty} \tilde{\alpha}_n z^n.$$

From its integral representation (3.8), the asymptotic expansions of P_+ are found to be

$$P_+(\xi) \sim k\left\{\frac{\tilde{b}_1}{(-i\xi)} + \frac{\tilde{b}_2}{(-i\xi)^2} + \ldots\right\} \quad \text{for} \quad \text{large } \xi \tag{A 5}$$

and

$$P_+(\pi\xi) = \tfrac{1}{2}k \sum_{p=0}^{\infty}\left[(-1)^p(-i\xi)^{p-\frac{1}{2}} \sum_{r=0}^{p} \nu_{rp}\{\log(-i\xi)\}^r + \mu_p(-i\xi)^p\right] + O[(-i\xi)^{n+\frac{1}{2}}\{\log(-i\xi)\}^{n+1}] \quad \text{for} \quad \text{small } \xi. \tag{A 6}$$

Here

$$\tilde{b}_n = \frac{(-i)^{n-\frac{5}{2}}}{4\sqrt{\pi}} \int_{C_-} \frac{|z| z^{n-1} (\coth |z| - 1)}{K_- z^{\frac{3}{2}}} dz,$$

$$\mu_p = \frac{(i)^p e^{-\frac{1}{4}i\pi}}{2\pi} \int_{C_-} \frac{p!\, z K_-^{-1}(\pi z) \coth(\pi z) + |z|_p K_-^{-1}(\pi z)}{z^{p+\frac{5}{2}}} dz \tag{A 7}$$

and

$$\nu_{rp} = \sum_{j=r}^{p} \frac{1}{j!} \beta_{p-j}\, {}^jC_r\, \pi^{j-r} |E_{j-r}|, \tag{A 8}$$

where ${}_nK_-^{-1}(\pi z)$ denotes the remainder after the $O(z^n)$ term in the small-z expansion (A 3), the E_n are the Euler numbers and the ${}^jC_r$ are the binomial coefficients.

From (A 2) and (A 5) we now get

$$\bar{g}_+(\xi) \sim k \left\{ \frac{b_1}{(-i\xi)^{\frac{3}{2}}} + \frac{b_2}{(-i\xi)^{\frac{5}{2}}} + \ldots \right\} \quad \text{for large } \xi, \tag{A 9}$$

where the b_n are determined by the relation

$$\frac{\tilde{b}_1 + \tilde{b}_2 z + \ldots}{1 + \pi\alpha_1 z + \pi^2 \alpha_2 z^2 + \ldots} = -2^{\frac{1}{2}}(b_1 + b_2 z + \ldots).$$

From (A 3) and (A 6) we get

$$\bar{g}_+(\xi) \sim -\tfrac{1}{2}k \sum_{p=0}^{n} \left[\tilde{A}_p (-i\xi)^{p-\frac{1}{2}} + (-i\xi)^p \sum_{r=0}^{p} \tilde{B}_{rp} \{\log(-i\xi)\}^r \right] + O[(-i\xi)^{n+\frac{1}{2}}] \quad \text{for small } \xi, \tag{A 10}$$

where the $\tilde{A}_p$ are functions of the β_n [in (A 4)] and the $\tilde{B}_{rp}$ are functions of the β_n, the μ_n [in (A 7)] and the ν_{rp} [in (A 8)]. It should be noted that terms like

$$\xi^{p-\frac{1}{2}} \{\log(-i\xi)\}^r$$

do not survive.

REFERENCES

Goldstein, S. 1960 *Lectures on Fluid Mechanics*. Interscience.

Libby, P. A. & Fox, H. 1963 Some perturbation solutions in laminar boundary-layer theory. Part 1. The momentum equation. *J. Fluid Mech.* **17**, 433.

Ludford, G. S. S. & Olunloyo, V. O. S. 1972*a* The forces on a flat plate in a Couette flow. *Z. angew. Math. Phys.* **23**, 115.

Ludford, G. S. S. & Olunloyo, V. O. S. 1972*b* Further results concerning the forces on a flat plate in a Couette flow. *Z. angew. Math. Phys.* to appear.

Van Dyke, M. 1964 Higher approximations in boundary-layer theory. Part 3. Parabola in uniform stream. *J. Fluid Mech.* **19**, 145.

Van Dyke, M. 1970 Entry flow in a channel. *J. Fluid Mech.* **44**, 813.

Wilson, S. D. R. 1971 Entry flow in a channel. Part 2. *J. Fluid Mech.* **46**, 787.